HHS Public Access

Metabolic Remodeling Precedes mTORC1-mediated Cardiac Hypertrophy

Giovanni E. Davogustto[a,1], **Rebecca L. Salazar**[a], **Hernan G. Vasquez**[a,2], **Anja Karlstaedt**[a,8], **William P. Dillon**[a], **Patrick H. Guthrie**[a,3], **Joseph R. Martin**[a,4], **Heidi Vitrac**[b], **Gina De La Guardia**[a,5], **Deborah Vela**[c], **Aleix Ribas-Latre**[d,6], **Corrine Baumgartner**[d,7], **Kristin Eckel-Mahan**[d], **Heinrich Taegtmeyer**[a,*]

[a]Division of Cardiology, Department of Internal Medicine, McGovern Medical School at The University of Texas Health Science Center at Houston, Houston, TX, USA

[b]Tosoh Bioscience LLC, King of Prussia, PA, USA

[c]Cardiovascular Pathology Research Laboratory, Texas Heart Institute at CHI St. Luke's Health, and the Department of Pathology and Laboratory Medicine, The University of Texas Health Science Center at Houston, Houston, TX, USA

[d]Center for Metabolic and Degenerative Diseases, Institute of Molecular Medicine, The University of Texas Health Science Center at Houston, Houston, TX, USA

Abstract

[*]Corresponding author at.:McGovern Medical School, The University of Texas Health Science Center at Houston, 6431 Fannin Street, MSB 1.220, Houston, TX 77030, USA. Heinrich.Taegtmeyer@uth.tmc.edu.

[1]Current affiliation: Division of Cardiovascular Medicine, Department of Medicine, Vanderbilt University Medical Center, Nashville, TN, USA

[2]Current affiliation: Department of Cardiovascular Surgery, Baylor College of Medicine, Houston, TX, USA

[3]Deceased

[4]Current affiliation: Department of Surgery, Icahn School of Medicine at Mount Sinai, New York, NY, USA

[5]Current affiliation: Edison Engineering Development Program, GE Healthcare, Chicago, IL, USA

[6]Current affiliation: Helmholtz Institute for Metabolic, Obesity and Vascular Research (HI-MAG) of the Helmholtz Zentrum München at the University of Leipzig and University Hospital Leipzig, Leipzig, Germany

[7]Current affiliation: Center for Cell and Gene Therapy, Texas Children's Hospital, Houston Methodist Hospital, and Baylor College of Medicine, Houston, TX, USA

[8]Current affiliation: Department of Cardiology, Smidt Heart Institute, Department of Biomedical Sciences, Cedars Sinai Medical Center, CA, USA

Rationale: The nutrient sensing mechanistic target of rapamycin complex 1 (mTORC1) and its primary inhibitor, tuberin (TSC2), are cues for the development of cardiac hypertrophy. The phenotype of mTORC1 induced hypertrophy is unknown.

Objective: To examine the impact of sustained mTORC1 activation on metabolism, function, and structure of the adult heart.

Methods and Results: We developed a mouse model of inducible, cardiac-specific sustained mTORC1 activation (mTORC1^{iSA}) through deletion of *Tsc2*. Prior to hypertrophy, rates of glucose uptake and oxidation, as well as protein and enzymatic activity of glucose 6-phosphate isomerase (GPI) were decreased, while intracellular levels of glucose 6-phosphate (G6P) were increased. Subsequently, hypertrophy developed. Transcript levels of the fetal gene program and pathways of exercise-induced hypertrophy increased. While hypertrophy did not progress to heart failure. We therefore examined the hearts of wild-type mice subjected to voluntary physical activity and observed early changes in GPI, followed by hypertrophy. Rapamycin prevented these changes in both models.

Conclusion: Activation of mTORC1 in the adult heart triggers the development of a non-specific form of hypertrophy which is preceded by changes in cardiac glucose metabolism.

Keywords

Stress-induced cardiac hypertrophy develops in response to two types of adaptation to chronic load [1]. The process can be either adaptive or maladaptive, and is considered a mechanism of the heart to normalize wall stress[2]. Each form of hypertrophy is thought to have its own distinct metabolic, structural, and functional profile. In adaptive hypertrophy rates of fatty acid oxidation are increased, while contractile function is preserved, or even augmented[3]. In maladaptive hypertrophy, rates of fatty acid oxidation are decreased in favor of glucose oxidation and glycolysis, concomitant with a return to the fetal gene program, while contractile function ultimately declines [2, 4].

A nodal point of hypertrophy signaling in mammalian cells is the nutrient-sensing mechanistic target of rapamycin complex 1 (mTORC1), an evolutionarily conserved kinase complex that links the insulin signaling pathway to the activation of anabolic processes and the inhibition of catabolic processes[5–7]. As such, mTORC1 is a key regulator of cellular metabolism and growth. The primary regulator of mTORC1 is the tuberous sclerosis complex, a heterotrimeric assembly of hamartin, tuberin (TSC2), and TBC1 Domain Family Member 7 (TBC1D7)[7, 8]. Tuberin, the active component of this assembly, functions as a GTPase-activating protein for the GTPase Ras homolog enriched in brain (Rheb). Multiple growth factor pathways converge at the tuberous sclerosis complex, resulting in phosphorylation of TSC2 which affects its activity. When TSC2 is inhibited, there is accumulation of GTP-bound Rheb, which strongly activates mTORC1. Due to its central role as a modulator of cellular growth, a possible link between mTORC1 activation and cardiac metabolism should provide new insights into mechanisms driving cardiac hypertrophy.

In the hemodynamically stressed heart *ex vivo*, we have previously observed that mTORC1 activation requires hexose 6-phosphate[9] and leads to contractile dysfunction[10]. Consistent with this observation, diverse pharmacologic and genetic models of mTORC1 inhibition protect against pathologic remodeling induced by pressure overload[11–14] or by metabolic stress[15]. On the one hand, this suggests that mTORC1 activation is a maladaptive process. On the other hand, multiple environmental exercise, and genetic models of physiologic hypertrophy also show mTORC1 activation. This would suggest that mTORC1 plays a role as an adaptive regulator, regardless whether hypertrophy is adaptive or maladaptive[16–18]. Furthermore, constitutive activation of mTORC1 produces no cardiac phenotype[19], while activation of mTORC1 in a model of congenital cardiac deletion of *Tsc2* results in cardiomyopathy[20]. Due to the presence of other stressors in most of the above-mentioned studies, it remains uncertain whether sustained mTORC1 activation in the adult heart, by itself, results in adaptive or maladaptive hypertrophy. The present study addresses this issue.

To determine the effects of sustained mTORC1 activation on metabolism, function, and structure of the adult heart, we developed a mouse model of inducible, cardiomyocyte-specific, sustained mTORC1 activation through knockdown of *Tsc2*. After observing similarities with physiologic cardiac hypertrophy in our genetic model, we next assessed cardiac metabolism, and mTORC1 activation in a mouse model of voluntary exercise and found that in both models hypertrophy is preceded by changes in cardiac glucose metabolism.

Methods

Detailed methods are provided in the Online Data Supplement.

Generation of a cardiac-specific, inducible, sustained mTORC1 activation mouse model through Tsc2 knockdown

Inducible, cardiac-specific sustained mTORC1 activation was achieved through *Tsc2* knockdown mice generated with an inducible MerCreMer system. TSC2$^{flox/flox}$ mice were produced and generously provided by Dr. Michael Gambello of Emory University School of Medicine [21]. This genetic strain has been validated as a method of conditional disruption of the *Tsc2* gene in neural tissue [22, 23], pancreas [24], and aorta [25]. TSC2$^{flox/flox}$ mice were crossbred with JAX B6.FVB(129)-TG(Myh6-Control/Esr1*)1 Jmk/J (stock #005657). The TSC2$^{flox/WT}$; αMHC-MerCreMer$^{+/−}$ progeny were backcrossed with the TSC2$^{flox/flox}$ mice to obtain TSC2$^{flox/flox}$; αMHC-MerCreMer$^{+/−}$ mice (mTORC1^{iSA}). TSC2$^{WT/WT}$; αMHC-MerCreMer$^{+/−}$ mice (Control) from a similar genetic background were used as controls to account for Cre-induced cardiac injury and transient cardiomyopathy [26, 27]. Recombination was induced at 5–6 weeks of age by the intraperitoneal administration of tamoxifen (TAM, 40mg/kg/day) for 21 days delivered during light cycle between 10:00 and 14:00 o'clock. Mice were housed on a 12-hour light/12-hour dark cycle in the Animal Care Center at McGovern Medical School, The University of Texas Health Science Center at Houston. Unless otherwise specified, the animals were fed a standard rodent laboratory diet *ad libitum* (LabDiet 5053).

Rapamycin treatment

Custom diets containing microencapsulated rapamycin or vehicle were prepared as previously described by Harrison *et al*[28]. mTORC1[iSA] mice were randomly assigned to rapamycin or vehicle diets. Short term diet treatment began at 10 weeks of age and continued until 12 weeks of age. Long term diet treatment began at 20 weeks and continued until 28 weeks of age.

Voluntary wheel exercise, basal activity monitoring, and rapamycin treatment

C57BL/6J (Jackson Labs, Bar Harbor, ME) male mice were housed singly in cages containing either 4-inch exercise wheels or infrared sensors, to measure voluntary exercise and basal activity respectively (STARR Life Sciences, Oakmont, PA). A first set of mice was subjected to short term voluntary exercise. On the 6th day, their hearts were harvested 4 hours after dark phase initiation, at peak activity, and after 12 hours of fasting. In a second set of experiments, mice subjected to the same 6 day exercise protocol were randomly assigned to being fed vehicle diet, or the microencapsulated rapamycin diet. On the 6th day, their hearts were harvested 4 hours after dark phase initiation, at peak activity, on the feeding state to ensure there would be enough circulating rapamycin levels for mTORC1 inhibition. On a third set of experiments, mice were subjected to 6 weeks of activity between free running animals fed the vehicle diet, free running animals fed the microencapsulated rapamycin diet, and non-exercised animals fed the vehicle diet. In this second cohort, the hearts were harvested between 9:00 and 11:00 o'clock. Activity data were collected with VitalView (STARR Life Sciences, Oakmont, PA) and analyzed by ClockLabs (Actimetrics, Wilmette, IL).

Echocardiography

Transthoracic echocardiography with pulse wave and tissue Doppler imaging was performed on male mice under isoflurane anesthesia using a VisualSonics Vevo 3100 platform with a MX550D probe, as described in the literature [29].

Western blotting

Protein homogenates were prepared from whole hearts as previously described[30]. Proteins of interest were detected via immunoblotting using horseradish peroxidase-conjugated secondary antibodies and chemiluminescence. Details of antibodies are provided in the supplement. Densitometry was performed using ImageJ v1.49 (National Institutes of Health, Bethesda, MD).

Quantitative reverse-transcript PCR

RNA was extracted from whole hearts using TRIzol®(Thermo Scientific, Wilmington DE) and the concentration and A260/A280 were measured by a NanoDrop 1000 spectrophotometer (Thermo Scientific, Wilmington DE). Total RNA was reverse transcribed into complementary DNA with iScriptTM Reverse Transcriptase (BioRad, Hercules CA). Using specific primers for each target transcript, real-time quantitative PCR was performed using SYBR-green and transcript levels were evaluated using the   Ct method, using TATA-box binding protein (*Tbp*) and Heat shock protein 90 alpha 1 (*Hsp90a1*) as normalization

controls, and expressed as a fold change over control, except for TSC2 transcript levels. Absolute quantification of *Tsc2* mRNA level was performed by the standard curve method, using cyclophilin A (*PpiA*)as a normalizer, with self-designed primers and TaqMan® probe. At least 3 biological replicates were averaged for each experiment. Validated BioRad PrimePCR assays were used for the majority of qPCR assays and are listed in Supplement Table2. The nucleotide sequences for probes as well as forward and reverse primers for the absolute quantitative PCR assays and pre-*miR222* are shown in Supplement Table 3.

DNA extraction and PCR

Hearts from 12 week-old mTORC1[iSA] and Control male mice were excised and cardiomyocytes isolated as previously described [31]. Then samples from adipose, brain, gastrocnemius, kidney, liver, and lungs, excised and flash frozen. Next, DNA was extracted from whole tissues or cardiomyocytes with Easy prep®(Sigma Aldrich, St Louis MO). Using 3 primers (Forward 1 5'-CCTCCTGCATGGAGTTGAGT-3', Forward 2 5'-CAGGCATGTCTGGAGTCTTG- 3', Reverse 5'-GCAGCAGGTCTGCAGTGAAT-3'), it is possible to identify the WT allele, floxed allele, and floxed allele after recombination. The product of the standard PCR was ran in a 2% agarose gel with ethidium bromide and PCR products visualized under UV light. The expected base pair size of the products are: 390bp, 434bp and 547bp for WT allele, floxed allele, and floxed allele after recombination, respectively.

Heart perfusions

Hearts from 12 week old mTORC1[iSA] and Control male mice were retrogradely perfused by the Langendorff method at 37 °C with Krebs-Henseleit bicarbonate buffer containing glucose (10 mM) and equilibrated with 95% CO_2/5% O_2 in the perfusionsystem previously described[32, 33] All experiments were done between the hours of 9:00 and 15:00 o'clock. Radioactive tracers [2-^{3}H]-glucose (50 μCi/L) and [U-^{14}C]-glucose (80 μCi/L) were used to measure rates of glucose uptake/phosphorylation and rates of glucose oxidation by the collection of [^{3}H]$_2$O and of [^{14}C]O$_2$ respectively in the coronary effluent, as described. At the end of the perfusions, beating hearts were freeze-clamped between aluminum blocks cooled in liquid N_2 and then stored at –80 °C[34]. These hearts were used for dry weight assessment in order to calculate rates of glucose uptake and oxidation.

Glucose 6-phosphate levels, and glucose 6-phosphate isomerase activity

G6P was determined enzymatically in extracts from freeze clamped hearts as previously described[10]. Glucose 6-phosphate isomerase (GPI) activity was measured by fructose 6-phosphate production from intracellular glucose 6-phosphate (G6P) determined colorimetrically with resorcinol as described by King[35].

Targeted Nucleotide Analysis using High-Performance Liquid Chromatography

Adenine nucleotide and nicotinamide adenine dinucleotide measurements were conducted in metabolite extracts from mouse hearts using high performance liquid chromatography (HPLC) separation and UV detection. Detailed reagents, methods, and instruments used

are detailed in the Supplement. Peak identification and quantification were conducted using Agilent OpenLab. Metabolite abundances were normalized by total protein concentration.

Histology

Hearts were excised, weighed and fixed overnight in 4% paraformaldehyde. Next, the fixed hearts were embedded in paraffin and sectioned at 5 μm thickness in the Histopathology Laboratory of McGovern Medical School at The University of Texas Health Science Center at Houston.

Cardiomyocyte area

Sections were stained with hematoxylin and eosin (H&E). Ten cardiomyocytes were analyzed per image, and ten images were taken per heart using a Motic AE2000 inverted phase microscope with attached Moticam 3 digital camera (Motic Optical, Richmond, BC, Canada). Images were analyzed using ImageJ v1.49 to measure cardiomyocyte cross-sectional diameter and area in cells with a single, central nucleus.

Interstitial fibrosis

Sections were stained with Masson's Trichrome. Fibrosis was measured using a Zeiss AxioCam HRc digital camera mounted to an Axiophot microscope and analyzed with Image Pro. An independent examiner (DV) was blinded to the origin of the samples.

Statistical analyses

All data are presented as mean +/− SEM, unless otherwise specified. The number of animals and replicates per experiment are indicated in the figure and/or figure legends. Specific statistical methods of comparison between groups are expanded upon in the figure legends and in the Online Data Supplement. A p value of < 0.05 was considered statistically significant. For Targeted Nucleotide Analysis using High-Performance Liquid Chromatography a FDR < 0.1 was considered statistically significant.

Results

Mouse model of inducible, cardiac-specific sustained mTORC1 activation.

Cardiomyocyte-specific sustained mTORC1 activation was achieved though partial *Tsc2* deletion using Cre-lox recombination. Recombination in the *Tsc2$^{flox/flox}$*; αMHC-MerCreMer$^{+/−}$ (mTORC1^{iSA}) mice was achieved by daily injections of tamoxifen (TAM, 40mg/kg body weight) for a period of 3 weeks, beginning at 5 weeks of age (Figure 1A). *Tsc2$^{WT/WT}$*; αMHC-MerCreMer$^{+/−}$(Control) mice were chosen as controls receiving the same course of daily TAM injections to account for potential cardiotoxic effects of the Cre recombinase[26, 36]. At 12 weeks of age, mTORC1^{iSA} mice displayed a ~3-fold decrease in TSC2 whole heart protein levels compared to control (Figure 1B). PCR of whole heart genomic DNA and RT-qPCR of whole heart RNA confirmed *Tsc2* recombination and reduced *Tsc2* expression (Supplement Figure 1A, B). Recombination of *Tsc2* by Cre was restricted to the cardiomyocyte (Supplement Figure 1C). Activation of mTORC1 was confirmed by an increase in the phosphorylation of mTOR, ribosomal protein S6

kinase (p70S6K), and eukaryotic translation initiation factor 4E-binding protein 1 (4EBP-1) (Figure 1C–E). Because the tuberous sclerosis complex is required for the mechanistic target of rapamycin complex 2 (mTORC2) activation[37], we investigated changes in phosphorylation on the target of mTORC2, Akt Ser 473 residue. Also, because mTORC1 can be activated through the insulin signaling pathway, we investigated Akt phosphorylation at the Thr 308 residue. There were no differences in phosphorylation between groups, indicating that changes in activation of mTORC2 nor the insulin signaling pathway were induced by knockdown of *Tsc2* (Figure 1 F–G).

With respect to other branches of mTORC1 signaling, there was an increase in the phosphorylation of Unc-51 like autophagy activating kinase (ULK-1) in hearts of mTORC1^{iSA} mice (Supplement Figure 1D), suggesting inhibition of autophagy with mTORC1 activation, as expected. However, there was no change in levels of mature SREBP-1 protein levels between both groups (Supplement Figure 1E). Furthermore, insulin receptor substrate 1 (IRS-1) phosphorylation (Ser 1101) was not different between both groups, suggesting no chronic activation of the insulin signaling pathway by p70S6K (Supplemental Figure 1F).

Concentric left ventricular hypertrophy in hearts of mTORC1^{iSA} mice.

Serial echocardiography showed no differences between control and mTORC1^{iSA} mice on left ventricular structure or systolic function at 12 weeks (Supplement Table 1). However, at 28 weeks of age, hearts of mTORC1^{iSA} mice had significantly smaller left ventricular internal diameter which led to a significant increase in relative wall thickness (RWT) (Table 1, and Supplement Figure 2). Systolic function was augmented in the mTORC1^{iSA} mice, but diastolic function did not differ between groups at 28 weeks of age.

Compared to controls, 28 week old mTORC1^{iSA} mice showed a significant increase in cardiomyocyte cross sectional area, with a corresponding increase in the heart weight to body weight (HW/BW) ratio (Figure 1H–I). Prior to Cre induction (5 weeks of age), and at 12 weeks of age, mTORC1^{iSA} and Control mice displayed similar cardiomyocyte cross-sectional areas and HW/BW ratios (Figure 1H–I). There was no difference in fibrosis, and the relatively high percentage of fibrosis observed in both groups was likely due to Cre-recombinase activity[38] (Figure 1J). Weight gain and long term survival did not differ between groups (Supplement Figure 3).

Gene expression after sustained mTORC1 activation in the heart.

Changes in gene expression in mTORC1^{iSA} mice at 28 weeks included increased transcript levels of the structural proteins myosin heavy chain β (*Myh7*) and skeletal α-actin (*Acta1*) (Figure 2A), as well as the biomarker brain natriuretic peptide (*Nppb*) (Figure 2B). Transcript levels of the early-response gene *c-Myc* were increased (Figure 2C). The expression of Cbp/p300 interacting transactivator 4 (*Cited4*) was also significantly increased at 28 weeks. (Figure 2D). The remainder of the fetal gene program[39] was unchanged at 28 weeks (Supplement Figure 4).

Metabolic remodeling precedes structural remodeling in hearts of mTORC1^{iSA} mice.

Rates of glucose uptake and oxidation, as assessed in retrogradely perfused hearts at 12 weeks, were reduced in mTORC1^{iSA} mice (Figure 3A–B), while levels of key proteins involved in glucose transport and phosphorylation (GLUT-1, GLUT-4, hexokinase 2) remained unchanged (Supplement Figure 5A–C).

Because we had previously shown that hexose 6-phosphate is required to activate mTORC1 in rat heart [9, 10], we measured G6P, the product of hexokinase-2 and the first committed metabolite in the glycolytic pathway. G6P levels were increased in hearts of mTORC1^{iSA} mice (Figure 3C), in spite of reduced rates of glucose uptake, suggesting a greatly reduced flux in the glycolytic pathway downstream from hexokinase. Phosphorylation of the cardiac isoform of phosphofructokinase-2 (PFKFB2), a chief regulator of glycolysis, was unchanged (Supplement Figure 5D).

Karlstaedt *et al.* recently examined the interaction between mTORC1 activation and glucose metabolism in the isolated working rat heart. In this study, the CardioGlyco computational model tracked flux and metabolite changes together with increase in cardiac work. It revealed that glycolysis was inhibited at the level of GPI[40]. Therefore, we interrogated GPI in the present genetic model and found a decrease in GPI enzyme activity at 12 weeks which persisted through 28 weeks of age (Figure 3D). Protein levels of GPI were decreased 5-fold in mTORC1^{iSA} mice as early as 12 weeks of age, which were attenuated at 28 weeks of age (Figure 3E). However, transcript levels of GPI at both 12 and 28 weeks did not differ (Figure 3F).

Despite the observed changes in glucose uptake and oxidation, there was no difference in the levels of ATP, ADP, and AMP in hearts of mTORC1^{iSA} mice (Figure 3G). Also, there was no changes in AMPK phosphorylation at Thr 172 between both groups (Supplement Figure 6A). To further investigate energy metabolism in hearts of mTORC1^{iSA} mice, we found no difference in levels of nicotinamide adenine dinucleotides (NAD$^+$/NADH). Similarly, to investigate possible disturbances in redox balance caused by a possible spillage of glucose into the oxidative pentose phosphate pathway, we measured nicotinamide adenine dinucleotide phosphates (NADP$^+$/NADPH). There were no significant changes in the levels of these metabolites either (Figure 3H). Collectively, these data support that hearts of mTORC1^{iSA} mice are not subjected to an energetic deficit or redox balance alterations.

Lastly, there was no difference between both groups in phosphorylation of acetyl-Co-A carboxylase (Supplement Figure 6B). This suggests a similar activity of this enzyme which catalyzes the carboxylation of acetyl-CoA into malonyl-CoA, a potent inhibitor of carnitine palmitoyltransferase 1 and, consequently, of fatty acid oxidation.

Induction of mTORC1 activation and metabolic changes by voluntary exercise.

At this point, we reasoned that the observed hypertrophy in the mTORC1 model possessed several features of adaptive hypertrophy, and went on to randomly assign wild-type C57BL/6J mice to either wheel running *ad libitum* (exercise), or to basal activity monitoring (sedentary). Mice housed with wheel-runners for 6 days displayed greater activity *per diem* than sedentary controls (Figure 4A) without a change in the HW/BW ratio (Figure

4B). After 6 days, hearts of animals subjected to exercise exhibited increased mTOR phosphorylation at Ser 2448 (Figure 4C). To evaluate if this mTORC1 activation was driven by TSC-2, we blotted for TSC-2 phosphorylation at Ser 1387, and it was decreased in hearts of mice subjected to exercise (Figure 4D). This residue is phosphorylated by AMPK, and its phosphorylation leads to inhibition of mTORC1 by TSC2 in response to energy deprivation[41]. There was also a decrease in GPI protein levels (Figure 4E). In spite of the decrease in GPI protein levels, GPI activity was increased (Figure 4F). Also, G6P levels were higher in exercised animals, but this difference did not reach statistical significance (Figure 4G). After short term exercise, ATP was not significantly changed but ADP and AMP were decreased (Supplement Figure 7A), and AMPK phosphorylation of Thr 172 was not significantly changed (Figure 4H). Nicotinamide adenine dinucleotides were all reduced (Supplement Figure 7B).

Effects of Rapamycin treatment in mTORC1^{iSA} and exercise models.

mTORC1^{iSA} mice were fed a diet containing encapsulated rapamycin to inhibit mTORC activity at two different points in the progression to cardiac hypertrophy (Figure 5A). The pharmacologic effects of rapamycin were confirmed with the assessment of phosphorylation of p70S6K in mTORC1^{iSA} mice at 28 weeks of age fed with chow containing rapamycin or vehicle for 8 weeks. As expected phosphorylation of p70S6K was reduced with rapamycin treatment (Supplement Figure 8).

The structural and functional changes seen in mTORC1^{iSA} mice at 28 weeks of age were prevented by rapamycin which was added to the diet for the last eight weeks of the experimental protocol. Echocardiography at 28 weeks showed decreased the left ventricular anterior wall thickness, systolic function, and relative wall thickness. Rapamycin treatment increased left ventricular internal diameter (Table 2). There was no significant difference in diastolic function with rapamycin treatment. Cardiomyocyte cross-sectional area and HW/BW ratio in rapamycin treated mTORC1^{iSA} mice did not differ from controls (Figure 5B–C). The changes in GPI protein levels observed at 12 weeks of age were also prevented by addition of rapamycin to the diet (Figure 5D).

Based on the increased phosphorylation of mTOR, decreased protein levels of GPI, and increased GPI activity observed in wild-type mice after six days of voluntary exercise, we also treated wild-type C57BL/6J mice with rapamycin during voluntary exercise. To evaluate if the metabolic changes observed in the short term exercise model could be prevented with rapamycin, we subjected mice to voluntary wheel exercise for 6 days, while assigning them to being fed with vehicle diet or rapamycin diet. The changes in GPI activity after the 6-day exercise protocol was prevented by addition of rapamycin to the diet (Figure 5E).

To probe if the remodeling induced by long term exercise could also be prevented with rapamycin, we then randomly assigned mice to three different groups: 1) a sedentary group fed the vehicle diet, 2) a voluntary exercise group fed the vehicle diet, and 3) a voluntary exercise group fed the rapamycin diet. After six weeks, HW/BW ratio was increased in voluntarily exercised mice fed the vehicle diet. Addition of rapamycin to the diet prevented this increase (Figure 5F). Body weight did not differ between the three groups nor did activity levels differ between the two diets of the voluntary exercise groups (Supplement

Figure 9A–B). In in hearts of mice subjected to long-term exercise there was no significant difference in mTORC1 phosphorilation (Supplement Figure 9C). Also, the decrease in GPI protein levels was no longer observed (Figure 5G). Regardless of unchanged GPI protein levels in this time point, GPI activity was also increased in voluntarily exercised mice fed the vehicle diet, and adding rapamycin to the diet prevented this increase (Figure 5H). With long term exercise there was a significant increase in ATP levels in mouse hearts, which was not seen with rapamycin treatment (Figure 5H). There was also a decrease in NAPD levels, although changes in NADP were not prevented with rapamycin treatment (Supplement Figure 10).

Discussion

We examined the impact of sustained mTORC1 activation on glucose metabolism, function and structure of the adult mouse heart and found that activation of mTORC1 triggers the development of a non-specific form of hypertrophy which is akin to exercise induced hypertrophy and preceded by changes in cardiac energy substrate metabolism. The findings merit a discussion of the different forms of cardiac hypertrophy and remodeling[2] before we consider possible mechanisms for the observed findings.

Physiologic vs. pathologic hypertrophy

With physiologic remodeling, there is no decrease in survival after a prolonged follow-up period, no increase in myocardial fibrosis, and no energetic deficit. This is also what we found in our genetic model. The metabolic remodeling, characterized by decreased glucose utilization, was also compatible with prior reports of physiologic changes in acute exercise bouts[3, 42]. However, the observed hypertrophy possessed distinct transcriptional changes associated with both, physiologic and pathologic, hypertrophy. Expression of the fetal isoforms of the structural proteins myosin and actin were increased without a change in the expression of the adult isoforms. Another transcriptional feature of maladaptive hypertrophy included increases in brain natriuretic peptide and *c-Myc*, while *Cited4* increased and the metabolic genes of the fetal gene program (both considered features of physiologic remodeling) remained unchanged.

Hence, our findings are consistent with previous models of mTORC1 activation in both physiologic and pathologic hypertrophy. Here it is also important to note that of the previously published studies of mTORC1 activation in the heart, the phenotype observed in our model was surprisingly different than a model of constitutive *Tsc2* deletion published by Taneike *et al*[20]. Constitutive deletion of *Tsc2* resulted in cardiomyocyte hypertrophy, cardiac dysfunction, and decreased survival. It is possible that the effect of mTORC1 sustained activation in the heart depends on developmental age. An argument against the differential effects of mTORC1 activation by age is the fact the constitutive active mTOR kinase mice do not develop a cardiac phenotype[19]. However, there could be a differential effect of mTORC1 activation by *Tsc2* deletion that has an age-dependent difference in effects on the heart. Another consideration to explain the differences is that a Cre control group was not included in Taneike's study, which makes it difficult to dissect the effects of mTORC1 from those of Cre activation in their model, or their interaction. This is

relevant because constitutive Cre activation in the heart is cardiotoxic and can cause dilated cardiomyopathy, although at a later age[43, 44].

mTORC1 activation by itself is neither adaptive or maladaptive

We propose that, instead of representing a switch for hypertrophy, the effects of mTORC1 activation in the adult heart are dependent on timing, duration of activation, and other stimuli. Thus mTORC1 is an enabler, or a hub of molecular signaling, facilitating metabolic remodeling first, and then hypertrophy, which is determined to be either physiologic or pathologic and the respective metabolic signature depending on the stimuli, and consequently other signaling pathways that are activated and/or inhibited concomitantly. We speculate that with pressure overload, mTORC1 activation synergizes with pathologic signaling cascades such as calcineurin, nuclear factor of activated T-cells (NFAT), mitogen-activated, and extracellular signal-regulated kinases (MAPK/ERK)[45], and leads to heart failure. However, in the mTORC1^{iSA} model, where the activation of mTORC1 occurs in early adulthood and is independent of such stresses, the hypertrophy exhibited appears to be non-pathologic. In this context, we note that the concept of hypertrophy being a continuum between physiologic and pathologic, rather than a dichotomous outcome has been raised before[46]. Our model, an intermediate phenotype in the physiologic end of this hypertrophy spectrum, supports this hypothesis.

It is also possible that the input affecting TSC2 activity, the degree of mTORC1 activation, as well as to which extent downstream targets of mTORC1 are preferentially activated and/or inhibited, determine the fate of hypertrophy in the heart, either pathologic or physiologic. Supporting this hypothesis, Oeing *et al*, recently showed that expression of S1365A mutation of TSC2 results in amplification of mTORC1 activity during ischemia reperfusion similar to WT controls subjected to ischemic preconditioning, both of which protect isolated hearts against ischemia reperfusion injury[47]. Prior models of pathologic and physiologic hypertrophy revealed 4EBP-1 hyperphosphorylation fold change of ~ 2, while p70S6K phosphorylation is ~2–3 fold for reported models of physiologic hypertrophy and variable between 2–10 fold in models of pathologic remodeling. Hyperphosphorylation of 4EBP-1 was in a similar range in our model. However, phosphorylation of p70S6K was remarkably greater in our model when compated to prior models of mTORC1 activation in the heart.

Metabolic changes precede structural changes

In earlier studies[10, 48–50], we showed that metabolic changes precede structural changes in cardiac remodeling. We argued that metabolism precedes, triggers and sustains functional and structural remodeling of the heart [51]and provides the building blocks of complex molecules[52]. Along these lines, Ritterhoff *et al.* demonstrated in isolated cardiomyocytes that when stimulated with phenylephrine, increased glucose consumption results in greater aspartate biosynthesis which leads to increased synthesis of nucleotides, RNA, proteins, and eventually cardiomyocyte hypertrophy[53].

Another link between metabolism and hypertrophy that we have demonstrated in heart muscle is the requirement of hexose6-phosphates for mTORC1 activation[9, 10]. Karlstaedt

et al. later showed that in heart muscle, GPI inhibition leads not only to mTORC1 activation but also shunts G6P into the pentose phosphate pathway (PPP)[40]. These observations are consistent with those from Roberts *et al.* in cardiomyocytes[54], but contrast with recent findings from Orozco *et al.*, suggesting that dihydroxyacetone phosphate is the signal that queus glucose availability to mTORC1 in HEK-293T cells [55].

Conversely, in the genetic model studied here, sustained mTORC1 activation caused accumulation of G6P associated with decreased GPI protein levels and enzymatic activity in the heart. This provides evidence of the feasibility of bidirectional crosstalk between metabolism and mTORC1 in heart muscle. Due to the decrease in glucose uptake and oxidation in the mTORC1^{iSA} model, we compared these changes with a known example of physiologic remodeling: voluntary exercise. After six days, the hearts of exercised wild-type mice displayed a decrease in GPI protein levels and a trend toward an increase in G6P akin to those observed in the mTORC1^{iSA} model. It was surprising, however, to find elevated GPI activity levels in this animals in spite of reduced protein levels. After six weeks, the hearts of voluntarily exercised wild-type mice showed a significant increase in heart size, and in GPI activity despite unchanged GPI protein levels. Rapamycin, a pharmacologic inhibitor of mTORC1, prevented the key metabolic and hypertrophic changes in both the voluntary exercise and the mTORC1^{iSA} models, suggesting a driving role of mTORC1 in both models.

Our findings support the observations by Gibb *et al.*[42], who used a kinase deficient 6-phosphofructo 2-kinase/fructose 2,6-biphosphatase (PFKFB2) to assess changes in myocardial glucose metabolism during exercise and found physiologic remodeling accompanied by an impairment of glycolytic flux during acute exercise. Similarly, a tight coupling of myocardial glucose uptake and oxidation caused by metformin prevents cardiac hypertrophy and improves systolic function in a model of pressure-overload[56]. The increase in ATP levels observed in hearts of mice subjected to long term voluntary exercise were prevented with rapamycin treatment. Taken together, these findings suggest that changes in energy providing metabolism are a consistent feature in the progression of cardiac hypertrophy.

Despite the insights from our study, our models have some limitations that require mentioning. First, it is challenging to conclude that mTORC1 activation by itself results in improved systolic function *in vivo*, due to potential differential sensitivity to isofluorane in mTORC1^{iSA} mice, as evidenced by lower heart rate in this group during the echocardiograms compared with controls. Also, the different conditions of hearts harvesting between short and long term exercise models, particularly feeding state in the long term exercise cohort, are potential reasons for not observing differences in mTORC1 activation in them and difficult the comparison of progression of metabolic changes. Lastly, the increased GPI activity with the 6 day exercise protocol might be due the fact that hearts animals are closer to the metabolic steady state achieved with training. Hence, our 6 day protocol might be an intermediate model of acute exercise bouts and long term training model.

In conclusion, cardiac-specific mTORC1 activation during early adulthood results in concentric hypertrophy without producing cardiac dysfunction. In the absence of external pathologic stimuli, which increase the heart's demand for glucose, sustained mTORC1

activation results in a decrease of GPI protein and activity, and a subsequent reduction in glycolytic flux. This metabolic remodeling precedes the structural changes observed in our cardiac-specific, inducible tuberin knockdown model and suggests that metabolic manipulation may serve as a target for modulating the hypertrophic response in the heart. Furthermore, we provide evidence that mTORC1 orchestrates metabolic remodeling that occurs in hearts with voluntary exercise.

The results presented here also encourage us to reexamine the spectrum of adaptive and maladaptive cardiac hypertrophy on a metabolic background. If reduction in GPI protein levels are sufficient to trigger hypertrophic remodeling, in which are the changes underlying the transition from the physiologic to pathologic remodeling?

Supplementary Material

Refer to Web version on PubMed Central for supplementary material.

Acknowledgments

References

[1]. Meerson FZ, Kapelko VI, The contractile function of the myocardium in two types of cardiac adaptation to a chronic load, Cardiology 57(4) (1972) 183–99. [PubMed: 4263006]

[2]. Hill JA, Olson EN, Cardiac plasticity, N Engl J Med 358(13) (2008) 1370–80. [PubMed: 18367740]

[3]. Fulghum K, Hill BG, Metabolic Mechanisms of Exercise-Induced Cardiac Remodeling, Frontiers in Cardiovascular Medicine 5(127) (2018).

[4]. van Bilsen M, van Nieuwenhoven FA, van der Vusse GJ, Metabolic remodelling of the failing heart: beneficial or detrimental?, Cardiovasc Res 81(3) (2009) 420–8. [PubMed: 18854380]

[5]. Saxton RA, Sabatini DM, mTOR Signaling in Growth, Metabolism, and Disease, Cell 169(2) (2017) 361–371. [PubMed: 28388417]

[6]. Sengupta S, Peterson TR, Sabatini DM, Regulation of the mTOR complex 1 pathway by nutrients, growth factors, and stress, Mol Cell 40(2) (2010) 310–22. [PubMed: 20965424]

[7]. Laplante M, Sabatini DM, mTOR signaling in growth control and disease, Cell 149(2) (2012) 274–93. [PubMed: 22500797]

[8]. Dibble CC, Elis W, Menon S, Qin W, Klekota J, Asara JM, Finan PM, Kwiatkowski DJ, Murphy LO, Manning BD, TBC1D7 is a third subunit of the TSC1-TSC2 complex upstream of mTORC1, Mol Cell 47(4) (2012) 535–46. [PubMed: 22795129]

[9]. Sharma S, Guthrie PH, Chan SS, Haq S, Taegtmeyer H, Glucose phosphorylation is required for insulin-dependent mTOR signalling in the heart, Cardiovasc Res 76(1) (2007) 71–80. [PubMed: 17553476]

[10]. Sen S, Kundu BK, Wu HC, Hashmi SS, Guthrie P, Locke LW, Roy RJ, Matherne GP, Berr SS, Terwelp M, Scott B, Carranza S, Frazier OH, Glover DK, Dillmann WH, Gambello MJ, Entman ML, Taegtmeyer H, Glucose regulation of load-induced mTOR signaling and ER stress in mammalian heart, J Am Heart Assoc 2(3) (2013) e004796.

[11]. Gao XM, Wong G, Wang B, Kiriazis H, Moore XL, Su YD, Dart A, Du XJ, Inhibition of mTOR reduces chronic pressure-overload cardiac hypertrophy and fibrosis, J Hypertens 24(8) (2006) 1663–70. [PubMed: 16877971]

[12]. Volkers M, Toko H, Doroudgar S, Din S, Quijada P, Joyo AY, Ornelas L, Joyo E, Thuerauf DJ, Konstandin MH, Gude N, Glembotski CC, Sussman MA, Pathological hypertrophy amelioration by PRAS40-mediated inhibition of mTORC1, Proc Natl Acad Sci U S A 110(31) (2013) 12661–6. [PubMed: 23842089]

[13]. Ranek MJ, Kokkonen-Simon KM, Chen A, Dunkerly-Eyring BL, Vera MP, Oeing CU, Patel CH, Nakamura T, Zhu G, Bedja D, Sasaki M, Holewinski RJ, Van Eyk JE, Powell JD, Lee DI, Kass DA, PKG1-modified TSC2 regulates mTORC1 activity to counter adverse cardiac stress, Nature 566(7743) (2019) 264–269. [PubMed: 30700906]

[14]. Oeing CU, Nakamura T, Pan S, Mishra S, Dunkerly-Eyring B, Kokkonen-Simon KM, Lin BL, Chen A, Zhu G, Bedja D, Lee DI, Kass DA, Ranek MJ, PKG1α Cysteine-42 Redox State Controls mTORC1 Activation in Pathological Cardiac Hypertrophy, Circ Res (2020).

[15]. Volkers M, Doroudgar S, Nguyen N, Konstandin MH, Quijada P, Din S, Ornelas L, Thuerauf DJ, Gude N, Friedrich K, Herzig S, Glembotski CC, Sussman MA, PRAS40 prevents development of diabetic cardiomyopathy and improves hepatic insulin sensitivity in obesity, EMBO Mol Med 6(1) (2014) 57–65. [PubMed: 24408966]

[16]. Ma Z, Qi J, Meng S, Wen B, Zhang J, Swimming exercise training-induced left ventricular hypertrophy involves microRNAs and synergistic regulation of the PI3K/AKT/mTOR signaling pathway, Eur J Appl Physiol 113(10) (2013) 2473–86. [PubMed: 23812090]

[17]. Kemi OJ, Ceci M, Wisloff U, Grimaldi S, Gallo P, Smith GL, Condorelli G, Ellingsen O, Activation or inactivation of cardiac Akt/mTOR signaling diverges physiological from pathological hypertrophy, J Cell Physiol 214(2) (2008) 316–21. [PubMed: 17941081]

[18]. Bezzerides VJ, Platt C, Lerchenmüller C, Paruchuri K, Oh NL, Xiao C, Cao Y, Mann N, Spiegelman BM, Rosenzweig A, CITED4 induces physiologic hypertrophy and promotes functional recovery after ischemic injury, JCI Insight 1(9) (2016) e85904.

[19]. Shen WH, Chen Z, Shi S, Chen H, Zhu W, Penner A, Bu G, Li W, Boyle DW, Rubart M, Field LJ, Abraham R, Liechty EA, Shou W, Cardiac restricted overexpression of kinase-dead mammalian target of rapamycin (mTOR) mutant impairs the mTOR-mediated signaling and cardiac function, J Biol Chem 283(20) (2008) 13842–9. [PubMed: 18326485]

[20]. Taneike M, Nishida K, Omiya S, Zarrinpashneh E, Misaka T, Kitazume-Taneike R, Austin R, Takaoka M, Yamaguchi O, Gambello MJ, Shah AM, Otsu K, mTOR Hyperactivation by Ablation of Tuberous Sclerosis Complex 2 in the Mouse Heart Induces Cardiac Dysfunction with the Increased Number of Small Mitochondria Mediated through the Down-Regulation of Autophagy, PLOS ONE 11(3) (2016) e0152628.

[21]. Hernandez O, Way S, McKenna J 3rd, Gambello MJ, Generation of a conditional disruption of the Tsc2 gene, Genesis 45(2) (2007) 101–6. [PubMed: 17245776]

[22]. Zeng LH, Rensing NR, Zhang B, Gutmann DH, Gambello MJ, Wong M, Tsc2 gene inactivation causes a more severe epilepsy phenotype than Tsc1 inactivation in a mouse model of tuberous sclerosis complex, Hum Mol Genet 20(3) (2011) 445–54. [PubMed: 21062901]

[23]. Way SW, McKenna J 3rd, Mietzsch U, Reith RM, Wu HC, Gambello MJ, Loss of Tsc2 in radial glia models the brain pathology of tuberous sclerosis complex in the mouse, Hum Mol Genet 18(7) (2009) 1252–65. [PubMed: 19150975]

[24]. Rachdi L, Balcazar N, Osorio-Duque F, Elghazi L, Weiss A, Gould A, Chang-Chen KJ, Gambello MJ, Bernal-Mizrachi E, Disruption of Tsc2 in pancreatic beta cells induces beta cell mass expansion and improved glucose tolerance in a TORC1-dependent manner, Proc Natl Acad Sci U S A 105(27) (2008) 9250–5. [PubMed: 18587048]

[25]. Cao J, Gong L, Guo DC, Mietzsch U, Kuang SQ, Kwartler CS, Safi H, Estrera A, Gambello MJ, Milewicz DM, Thoracic aortic disease in tuberous sclerosis complex: molecular pathogenesis and potential therapies in Tsc2+/− mice, Hum Mol Genet 19(10) (2010) 1908–20. [PubMed: 20159776]

[26]. Koitabashi N, Bedja D, Zaiman AL, Pinto YM, Zhang M, Gabrielson KL, Takimoto E, Kass DA, Avoidance of transient cardiomyopathy in cardiomyocyte-targeted tamoxifen-induced MerCreMer gene deletion models, Circ Res 105(1) (2009) 12–5. [PubMed: 19520971]

[27]. Bersell K, Choudhury S, Mollova M, Polizzotti BD, Ganapathy B, Walsh S, Wadugu B, Arab S, Kuhn B, Moderate and high amounts of tamoxifen in alphaMHC-MerCreMer mice induce a

DNA damage response, leading to heart failure and death, Dis Model Mech 6(6) (2013) 1459–69. [PubMed: 23929941]

[28]. Harrison DE, Strong R, Sharp ZD, Nelson JF, Astle CM, Flurkey K, Nadon NL, Wilkinson JE, Frenkel K, Carter CS, Pahor M, Javors MA, Fernandez E, Miller RA, Rapamycin fed late in life extends lifespan in genetically heterogeneous mice, Nature 460(7253) (2009) 392–5. [PubMed: 19587680]

[29]. Respress JL, Wehrens XHT, Transthoracic Echocardiography in Mice, J Vis Exp (39) (2010).

[30]. Rees ML, Subramaniam J, Li Y, Hamilton DJ, Frazier OH, Taegtmeyer H, A PKM2 signature in the failing heart, Biochem Biophys Res Commun 459(3) (2015) 430–6. [PubMed: 25735978]

[31]. O'Connell TD, Rodrigo MC, Simpson PC, Isolation and culture of adult mouse cardiac myocytes, Methods Mol Biol 357 (2007) 271–96. [PubMed: 17172694]

[32]. Taegtmeyer H, Hems R, Krebs HA, Utilization of energy-providing substrates in the isolated working rat heart, Biochem J 186(3) (1980) 701–11. [PubMed: 6994712]

[33]. Goodwin GW, Taylor CS, Taegtmeyer H, Regulation of energy metabolism of the heart during acute increase in heart work, J Biol Chem 273(45) (1998) 29530–9. [PubMed: 9792661]

[34]. Wollenberger A, Ristau O, Schoffa G, [A simple technic for extremely rapid freezing of large pieces of tissue], Pflugers Arch Gesamte Physiol Menschen Tiere 270 (1960) 399–412.

[35]. King J, Glucosephosphate Isomerase, in: Bergmeyer HU (Ed.), Methods of Enzymatic Analysis., Verlag- Chemie International, Deerfield Beach, FL 1974.

[36]. Buerger A, Rozhitskaya O, Sherwood MC, Dorfman AL, Bisping E, Abel ED, Pu WT, Izumo S, Jay PY, Dilated cardiomyopathy resulting from high-level myocardial expression of Cre-recombinase, J Card Fail 12(5) (2006) 392–8. [PubMed: 16762803]

[37]. Huang J, Dibble CC, Matsuzaki M, Manning BD, The TSC1-TSC2 complex is required for proper activation of mTOR complex 2, Mol Cell Biol 28(12) (2008) 4104–15. [PubMed: 18411301]

[38]. Lexow J, Poggioli T, Sarathchandra P, Santini MP, Rosenthal N, Cardiac fibrosis in mice expressing an inducible myocardial-specific Cre driver, Dis Model Mech 6(6) (2013) 1470–6. [PubMed: 23929940]

[39]. Depre C, Shipley GL, Chen W, Han Q, Doenst T, Moore ML, Stepkowski S, Davies PJA, Taegtmeyer H, Unloaded heart in vivo replicates fetal gene expression of cardiac hypertrophy, Nature Medicine 4(11) (1998) 1269–1275.

[40]. Karlstaedt A, Khanna R, Thangam M, Taegtmeyer H, Glucose 6-Phosphate Accumulates via Phosphoglucose Isomerase Inhibition in Heart Muscle, Circ Res 126(1) (2019) 60–74. [PubMed: 31698999]

[41]. Inoki K, Zhu T, Guan KL, TSC2 mediates cellular energy response to control cell growth and survival, Cell 115(5) (2003) 577–90. [PubMed: 14651849]

[42]. Gibb AA, Epstein PN, Uchida S, Zheng Y, McNally LA, Obal D, Katragadda K, Trainor P, Conklin DJ, Brittian KR, Tseng MT, Wang J, Jones SP, Bhatnagar A, Hill BG, Exercise-Induced Changes in Glucose Metabolism Promote Physiological Cardiac Growth, Circulation 136(22) (2017) 2144–2157. [PubMed: 28860122]

[43]. Pugach EK, Richmond PA, Azofeifa JG, Dowell RD, Leinwand LA, Prolonged Cre expression driven by the α-myosin heavy chain promoter can be cardiotoxic, J Mol Cell Cardiol 86 (2015) 54–61. [PubMed: 26141530]

[44]. Rehmani T, Salih M, Tuana BS, Cardiac-Specific Cre Induces Age-Dependent Dilated Cardiomyopathy (DCM) in Mice, Molecules 24(6) (2019).

[45]. Weeks KL, McMullen JR, The athlete's heart vs. the failing heart: can signaling explain the two distinct outcomes?, Physiology (Bethesda) 26(2) (2011) 97–105. [PubMed: 21487028]

[46]. Dorn GW, The Fuzzy Logic of Physiological Cardiac Hypertrophy, Hypertension 49(5) (2007) 962–970. [PubMed: 17389260]

[47]. Oeing CU, Jun S, Mishra S, Dunkerly-Eyring B, Chen A, Grajeda MI, Tahir U, Gerszten RE, Paolocci N, Ranek MJ, Kass DA, MTORC1-Regulated Metabolism Controlled by TSC2 Limits Cardiac Reperfusion Injury, Circulation Research 0(0).

[48]. Zhong M, Alonso CE, Taegtmeyer H, Kundu BK, Quantitative PET imaging detects early metabolic remodeling in a mouse model of pressure-overload left ventricular hypertrophy in vivo, J Nucl Med 54(4) (2013) 609–15. [PubMed: 23426760]

[49]. Kundu BK, Zhong M, Sen S, Davogustto G, Keller SR, Taegtmeyer H, Remodeling of glucose metabolism precedes pressure overload-induced left ventricular hypertrophy: review of a hypothesis, Cardiology 130(4) (2015) 211–20. [PubMed: 25791172]

[50]. Hamirani YS, Kundu BK, Zhong M, McBride A, Li Y, Davogustto GE, Taegtmeyer H, Bourque JM, Noninvasive Detection of Early Metabolic Left Ventricular Remodeling in Systemic Hypertension, Cardiology 133(3) (2016) 157–62. [PubMed: 26594908]

[51]. Taegtmeyer H, Golfman L, Sharma S, Razeghi P, Van Arsdall M, Linking Gene Expression to Function: Metabolic Flexibility in the Normal and Diseased Heart, Annals of the New York Academy of Sciences 1015(1) (2004) 202–213. [PubMed: 15201161]

[52]. Davogustto G, Taegtmeyer H, The changing landscape of cardiac metabolism, J Mol Cell Cardiol 84 (2015) 129–32. [PubMed: 25937535]

[53]. Ritterhoff J, Young S, Villet O, Shao D, Neto FC, Bettcher LF, Hsu Y-WA, Kolwicz SC, Raftery D, Tian R, Metabolic Remodeling Promotes Cardiac Hypertrophy by Directing Glucose to Aspartate Biosynthesis, Circulation Research 126(2) (2020) 182–196. [PubMed: 31709908]

[54]. Roberts DJ, Tan-Sah VP, Ding EY, Smith JM, Miyamoto S, Hexokinase-II positively regulates glucose starvation-induced autophagy through TORC1 inhibition, Mol Cell 53(4) (2014) 521–33. [PubMed: 24462113]

[55]. Orozco JM, Krawczyk PA, Scaria SM, Cangelosi AL, Chan SH, Kunchok T, Lewis CA, Sabatini DM, Dihydroxyacetone phosphate signals glucose availability to mTORC1, Nature Metabolism (2020).

[56]. Li J, Min zuk K, Massey JC, Howell NL, Roy RJ, Paul S, Patrie JT, Kramer CM, Epstein FH, Carey RM, Taegtmeyer H, Keller SR, Kundu BK, Metformin Improves Cardiac Metabolism and Function, and Prevents Left Ventricular Hypertrophy in Spontaneously Hypertensive Rats, Journal of the American Heart Association 9(7) (2020) e015154.

Highlights

- Sustained mTORC1 activation via inducible tuberin knockdown in the heart results in concentric hypertrophy without producing cardiac dysfunction.

- Sustained mTORC1 activation in the heart results in decrease of glucose 6-phosphate isomerase protein and activity. This is accompanied by a reduction of glycolytic flux that precedes hypertrophy.

- In short term voluntary exercise there is a similar activation of mTORC1 via reduced TSC2 phosphorylation at Serine 1387, and a decrease in glucose 6-phosphate isomerase protein levels, but with increased activity which is prevented with rapamycin treatment.
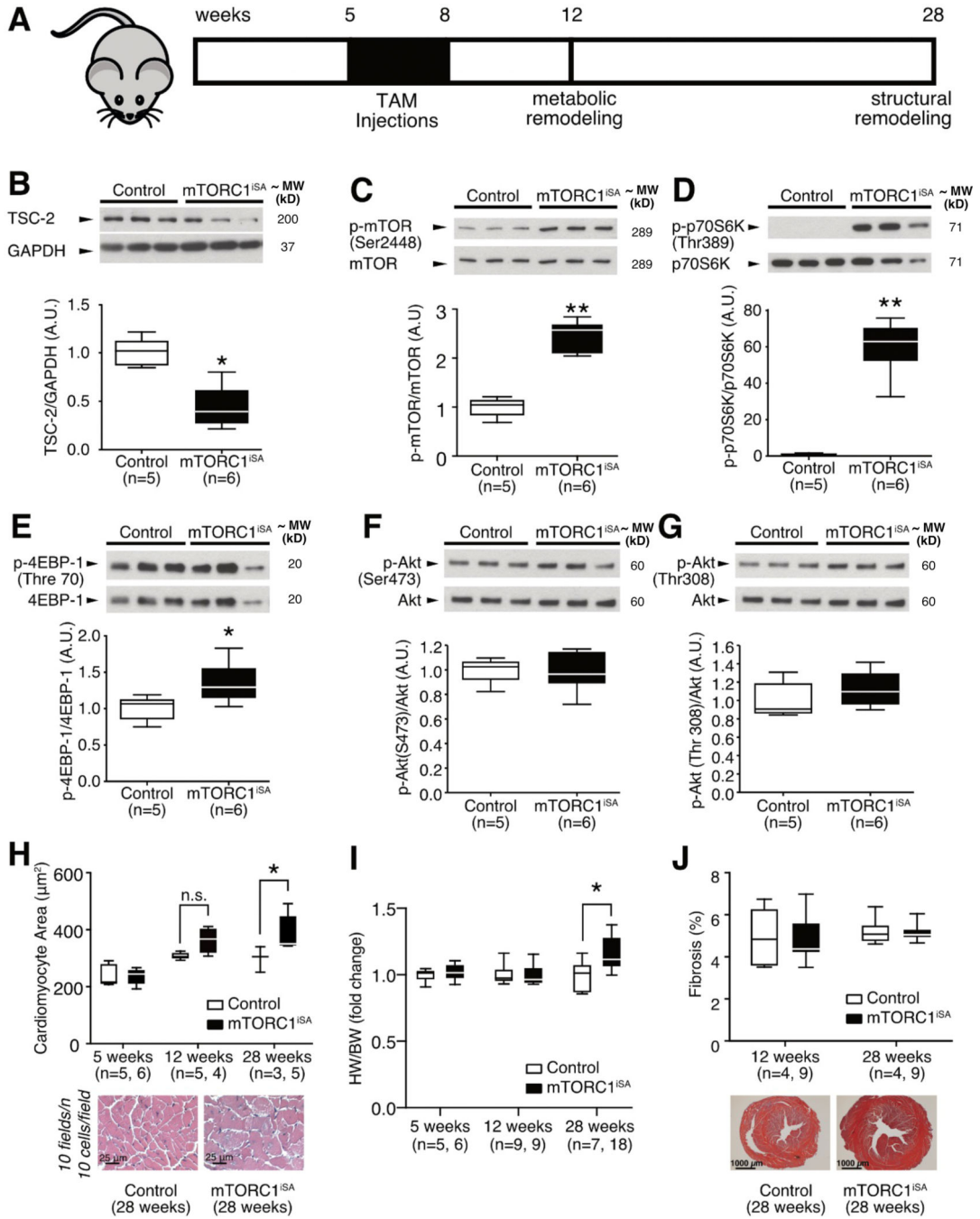
Figure 1. TSC2 knockdown produces sustained mTORC1 activation in adult mouse hearts leading to cardiac hypertrophy without increased fibrosis.

(A) Model of sustained mTORC1 activation via *Tsc2* knockdown, timeline of Cre-recombinase induction, and timepoints for assessment of metabolic and structural remodeling. (B) TSC2 protein levels in mTORC1[iSA] mouse hearts at 12 weeks were decreased (n=5 Control and 6 mTORC1[iSA] mice). (C) mTOR phosphorylation at Ser2448 was increased in mTORC1[iSA] mouse hearts at 12 weeks (n=5 Control and 6 mTORC1[iSA] mice). (D) Phosphorylation of p70S6K at Thr389 was increased in mTORC1[iSA] mouse hearts at 12 weeks (n=5 Control and 6 mTORC1[iSA] mice). (E) 4EBP-1 was

hyperphosphorylated at Thr70 in mTORC1^{iSA} mouse hearts at 12 weeks (n=5 Control and 6 mTORC1^{iSA} mice). (F) Akt phosphorylation at Ser473 was unchanged in mTORC1^{iSA} mouse hearts at 12 weeks (n=5 Control and 6 mTORC1^{iSA} mice). (G) Akt phosphorylation at Ser308 was unchanged in mTORC1^{iSA} mouse hearts at 12 weeks(n=5 Control and 6 mTORC1^{iSA} mice). (H) Cardiomyocyte cross-sectional areas pre-recombination (5 weeks, n=5 Control and 6 mTORC1^{iSA} mice), and post-recombination (12 weeks [n=5 Control and 4 mTORC1^{iSA} mice], and 28 weeks [n=3 Control and 4 mTORC1^{iSA} mice]), with representative H/E at 28 weeks. (I) Heart Weight to Body Weight (HW/BW) ratios from Control and mTORC1^{iSA} mice pre-recombination (5 weeks, n=5 Control and 6 mTORC1^{iSA} mice), and post-recombination (12 weeks [n=9 mice per group], and 28 weeks [n=7 Control and 18 mTORC1^{iSA} mice]). (J). Fibrosis in hearts of Control and mTORC1^{iSA} post-recombination (12 weeks [n=4 Control and 9 mTORC1^{iSA} mice], and 28 weeks [n=4 Control and 9 mTORC1^{iSA} mice]), with representative Masson Trichrome at 28 weeks. Statistical significance was calculated using unpaired two-tailed Student's t test (B-G), and two-way ANOVA with Bonferroni's multiple comparisons test (H-J); *p<0.05, **p<0.01.
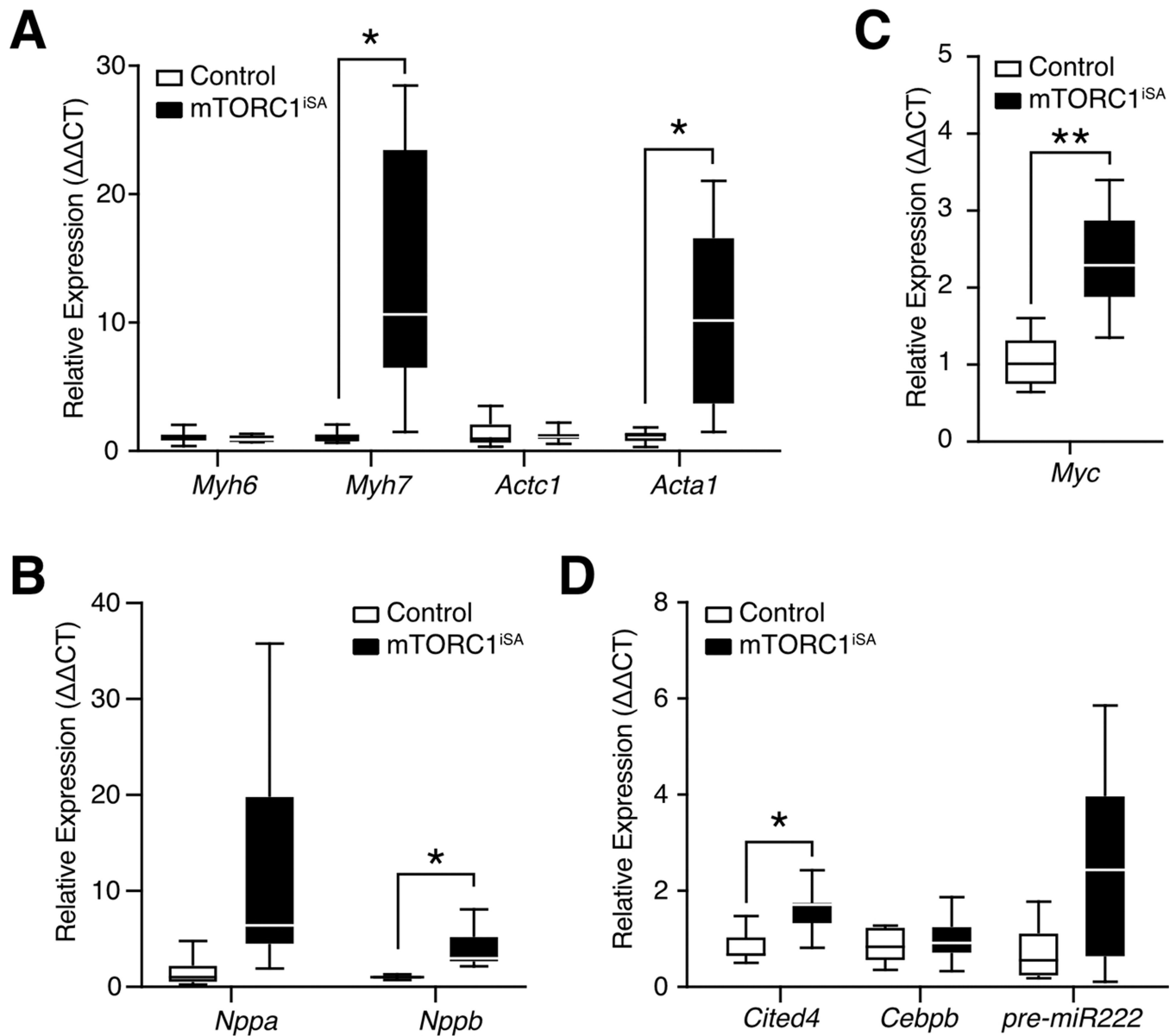
Figure 2. Sustained mTORC1 activation in adult mouse hearts results in transcriptional changes associated with both adaptive and maladaptive hypertrophy.
(A) The fetal isoforms of myosin heavy chain (*Myh7*) and actin (*Acta1*) were upregulated at 28 weeks in mTORC1[iSA] mice (n= 9 mice per group). (B) Brain natriuretic peptide (*Nppb*) was upregulated at 28 weeks in mTORC1[iSA] mice (n= 9 mice per group). (C) *c-Myc* expression was upregulated at 28 weeks in mTORC1[iSA] mice (n= 9 mice per group). (D) *Cited4* was upregulated at 28 weeks in mTORC1[iSA] mice (n= 9 mice per group). Statistical significance was calculated using unpaired two-tailed Student's t test with correction for multiple comparisons using the Holm-Sidak method; $*p<0.05$, $**p<0.01$. *Myh6*, myosin heavy chain α; *Myh7*, myosin heavy chain β; *Actc1*, cardiac α-actin; *Acta1*, skeletal α-actin; *Cited4*, Cbp/p300 interacting transactivator 4; *Cebpb*, CCAAT/enhancer-binding protein β; *miR222*, pre-miRNA 222; *Myc*, c-Myc; *Nppa*, atrial natriuretic protein; *Nppb*, brain natriuretic protein.
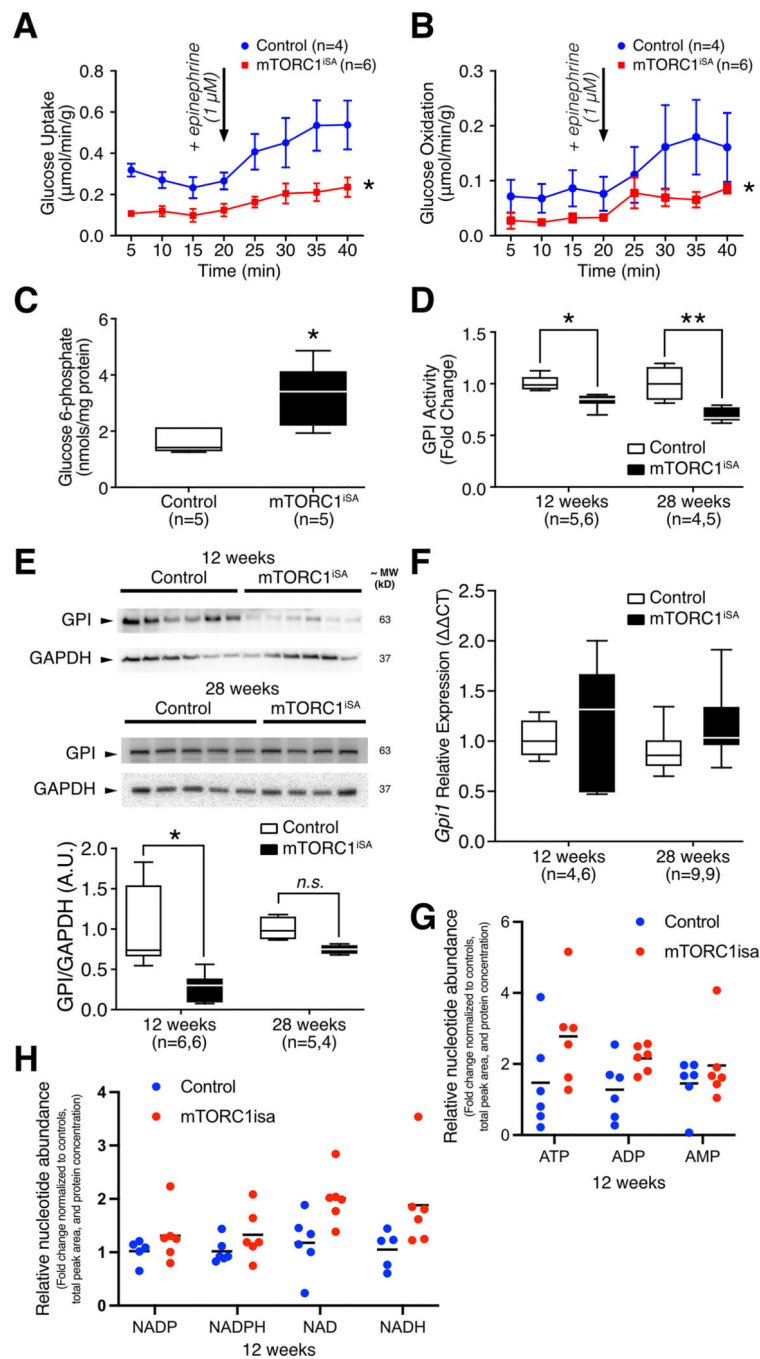
Figure 3. Sustained mTORC1 activation in adult mouse hearts induces metabolic remodeling in mTORC1^{iSA} mice at 12 weeks.

(A) Rates of glucose uptake and (B) glucose oxidation were decreased in retrogradely perfused mTORC1^{iSA} mouse hearts at 12 weeks (n= 4 Control and 6 mTORC1^{iSA} mice). (C) G6P metabolite levels were elevated in the heart muscle of mTORC1^{iSA} mice at 12 weeks (n=5 mice per group). (D) GPI activity is depressed at 12 weeks (n= 5 Control and 6 mTORC1^{iSA} mice) in mTORC1^{iSA} and this decrease is sustained through 28 weeks (n= 4 Control and 6 mTORC1^{iSA} mice). (E) GPI protein levels measured in mTORC1^{iSA} mouse hearts at 12 weeks (n=6 mice per group) were decreased and this decrease is attenuated

at 28 weeks (n= 5 Control and 4 mTORC1^{iSA} mice). (F) There was no change in the transcription of GPI at either 12 weeks (n= 4 Control and 6 mTORC1^{iSA} mice) or 28 weeks (n=9 mice per group). (G and H) Levels of ATP, ADP, and AMP, as well as Nicotinamide adenine dinucleotides were similar in mTORC1^{iSA} than in control mouse hearts at 12 weeks (n=6 mice per group). Nucleotide abundance is expressed as fold-change from control, and was normalized by total peak area and protein concentration. Statistical significance was calculated using two-way ANOVA (A and B), unpaired two-tailed Student's t test (C), two-way ANOVA with Bonferroni's multiple comparisons test (D and F), unpaired two-tailed Student's t test with correction for multiple comparisons using a FDR of 0.1 (G-H); *p<0.05, **p<0.01.
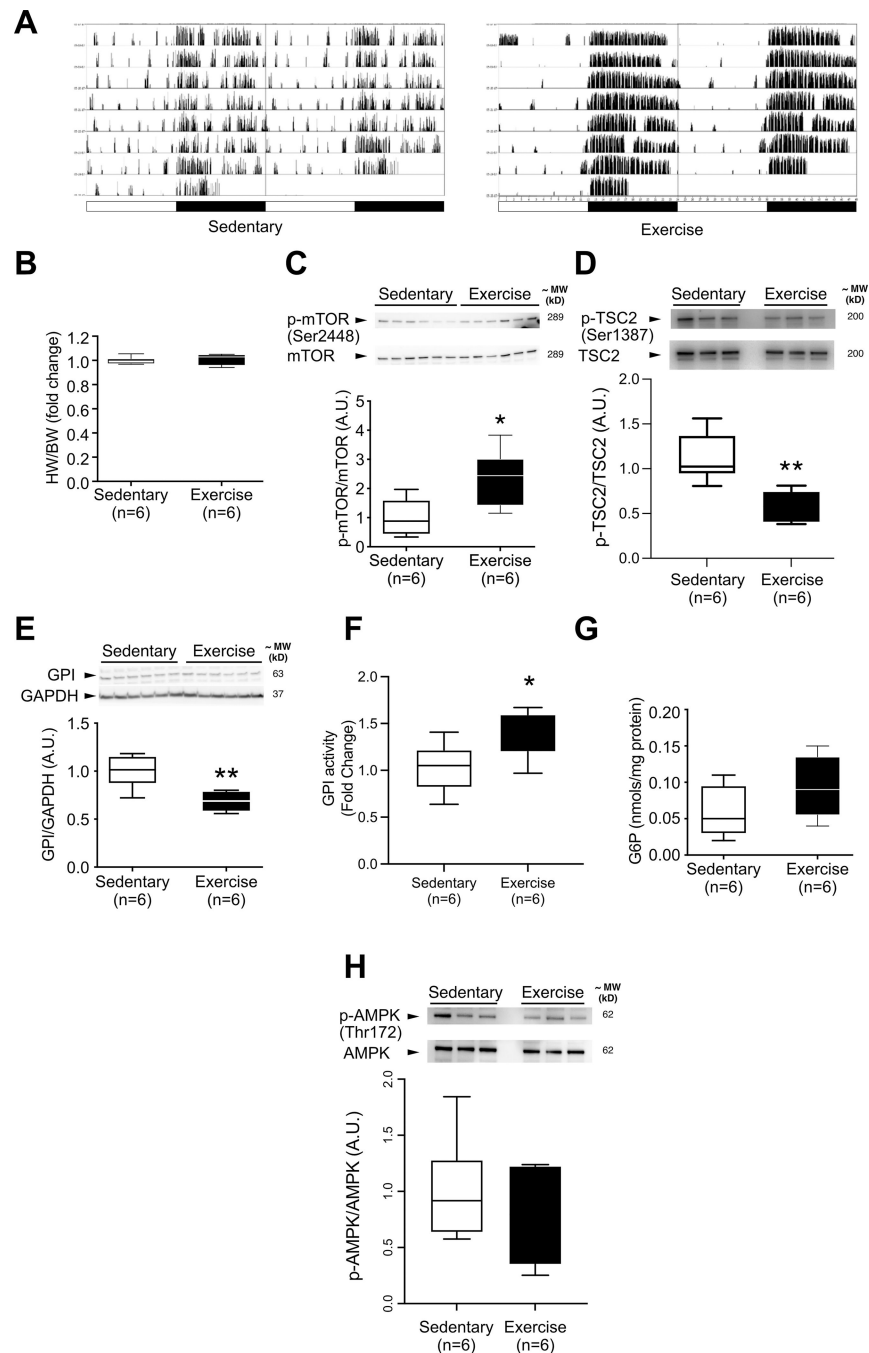
Figure 4. GPI protein levels are decreased in parallel with increased mTOR phosphorylation during acute exercise after six days of voluntary exercise training.

(A) Representative home cage circadian activity of sedentary and voluntarily exercising C57BL6/J mice, as measured by infrared motion detector (left columns) and wheel runner reed switches (right columns). (B) Heart weight to body weight ratio does not differ between groups after 6 days of voluntary exercise (n=6 mice per group). (C) mTOR phosphorylation at Ser2448 is increased in voluntarily exercised C57BL6/J mice (n=6 mice per group). (D) TSC2 phosphorylation at Ser1387 is decreased in voluntarily exercised C57BL6/J mice (n=6 mice per group). (E) GPI protein levels are decreased in the hearts of voluntarily

exercised C57BL6/J mice (n=6 mice per group). (F) GPI activity is increased in the hearts of voluntarily exercised C57BL6/J mice (n=6 mice per group) (G) G6P levels in the hearts of voluntarily exercised mice are not significantly increased (n=6 mice per group). (H) AMPK phosphorylation at Thr172 is unchanged in voluntarily exercised C57BL6/J mice (n=6 mice per group). Statistical significance was calculated using unpaired two-tailed Student's t test; *p<0.05, ** p<0.01.
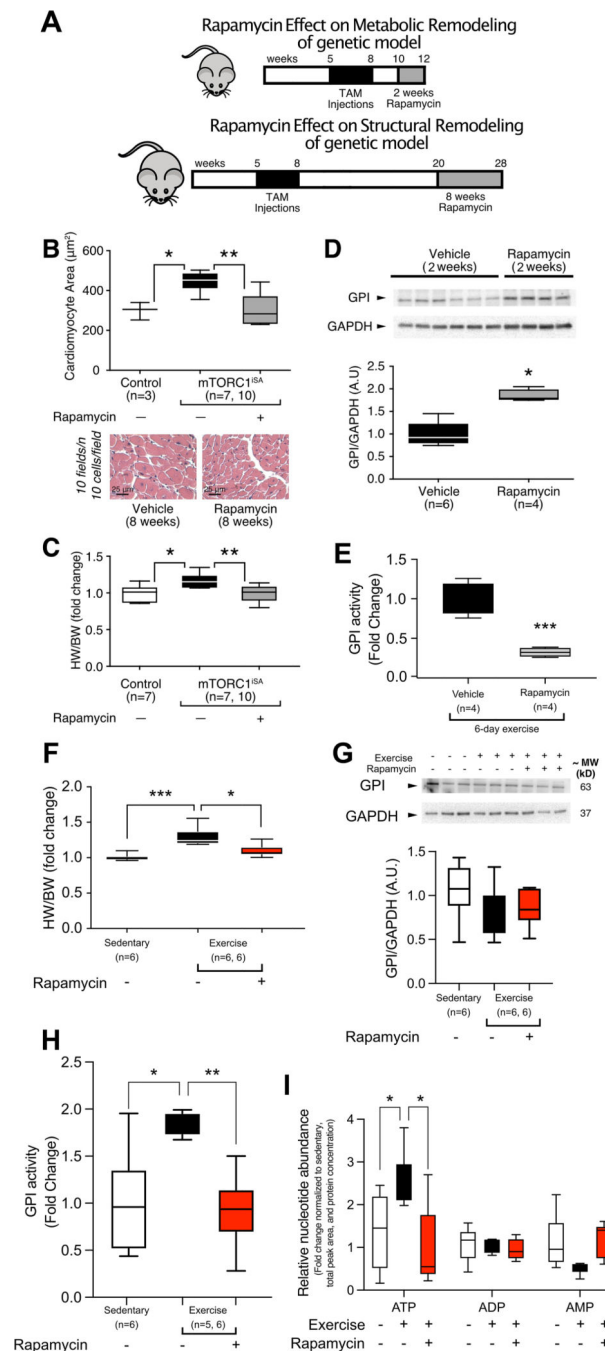
Figure 5. Rapamycin treatment prevents metabolic and structural remodeling observed in both mTORC1^iSA and exercise models.

(A) Model of sustained mTORC1 activation via *Tsc2* knockdown, timeline of treatment with rapamycin prior to metabolic and structural remodeling. The increases in cardiomyocyte area (B) and HW/BW ratio (C) seen in mTORC1^iSA mice at 28 weeks were prevented when fed a diet containing rapamycin for 8 weeks (n=3 and 7 Control mice in B and C, respectively, 7 mTORC1^iSA mice treated with vehicle and 10 mTORC1^iSA treated with rapamycin). (D) Two weeks of rapamycin in the diet prevented the decrease of GPI protein levels seen in hearts of mTORC1^iSA mice at 12 weeks (n=6 Vehicle treated and 4 rapamycin

treated mice). (E) Rapamycin in the diet during the six days exercise protocol prevevents GPI activity increase in hearts of voluntarily exercised C57BL6/J mice (n=4 mice per group). (F) After 6 weeks of voluntary exercise, HW/BW ratio increases in C57BL/6 mice similar to the HW/BW increase seen in mTORC1^{iSA} mice, and rapamycin diet during this 6 week period prevented this increase (n=6 mice per group). (G) After 6 weeks of voluntary exercise, GPI protein levels in hearts of C57BL/6 mice were unchanged. Rapamycin, diet during this 6 week period did not cause further changes in GPI (n=6 mice per group). (F) After 6 weeks of voluntary exercise, GPI activity increases in C57BL/6 mice similar and rapamycin diet during this 6 week period prevented this increase (n=6 mice per group). (I) After 6 weeks of voluntary exercise, ATP levels were increased in hearts of C57BL/6 mice, and rapamycin diet during this 6 week period prevented this increase, (n=6 mice per group). Statistical significance was calculated using one-way ANOVA with Tukey's multiple comparisons test (B, C, F-H), unpaired two-tailed Student's t test (D-E), and one-way ANOVA with Tukey's multiple comparisons test using a FDR of 0.1 (I), (*$p < 0.05$ orFDR < 0.1, ** $p < 0.01$, *** $p < 0.001$)

Table 1.

Echocardiographic parameters in mTORC1^{iSA} and Control mice at 28 weeks.

Parameter	Control (n=8)	mTORC1^{iSA} (n=9)
LVAWd (mm)	0.99 ± 0.06	1.12 ± 0.05
LVAWs (mm)	1.44 ± 0.08	1.63 ± 0.06
LVIDd (mm)	3.97 ± 0.07	3.61 ± 0.09 **
LVIDs (mm)	2.81 ± 0.05	2.31 ± 0.07 **
LVPWd (mm)	0.96 ± 0.06	1.01 ± 0.08
LVPWs (mm)	1.35 ± 0.05	1.42 ± 0.10
EF (%)	56.01 ± 2.07	66.38 ± 1.80 **
FS (%)	28.92 ± 1.37	36.04 ± 1.39 **
Heart rate (bpm)	433.9 ± 16.48	384.8 ± 7.35 *
Relative Wall Thickness	0.49 ± 0.02	0.59 ± 0.03 *
E/A	1.46 ± 0.11	1.83 ± 0.13
E/e'	33.94 ± 3.30	28.23 ± 3.24
IVRT/RR	0.15 ± 0.01	0.15 ± 0.01

LVAWd: Left Ventricular Anterior Wall in diastole. LVAWs: Left Ventricular Anterior Wall in systole. LVIDd: Left Ventricular Internal Diameter in diastole. LVIDs: Left Ventricular Internal Diameter in systole. LVPWd: Left Ventricular Posterior Wall in diastole. LVPWs: Left Ventricular Posterior Wall in systole. EF: Ejection Fraction. FS: Fractional Shortening. Statistical significance was calculated using unpaired two-tailed Student's t test;

*
$p < 0.05$

**
$p < 0.01$.

Table 2.

Echocardiographic parameters in mTORC1^{iSA} mice fed either rapamycin or vehicle diet at 28 weeks.

Parameter	Vehicle (n=6)	Rapamycin (n=6)
LVAWd (mm)	1.18 ± 0.06	0.87 ± 0.07 **
LVAWs (mm)	1.70 ± 0.07	1.28 ± 0.10 **
LVIDd (mm)	3.42 ± 0.19	3.99 ± 0.16 *
LVIDs (mm)	2.06 ± 0.19	2.86 ± 0.23 *
LVPWd (mm)	1.04 ± 0.06	0.99 ± 0.10
LVPWs (mm)	1.50 ± 0.09	1.39 ± 0.13
EF (%)	73.76 ± 2.93	57.39 ± 4.65 *
FS (%)	42.13 ± 2.38	30.17 ± 3.09 *
Heart rate (bpm)	382.3 ± 13.49	413.7 ± 9.82
Relative Wall Thickness	0.66 ± 0.06	0.47 ± 0.04 *
E/A [a]	1.90 ± 0.08	1.45 ± 0.25
E/e'	33.97 ± 1.71	38.04 ± 4.31
IVRT/RR	0.14 ± 0.02	0.14 ± 0.01

LVAWd: Left Ventricular Anterior Wall in diastole. LVAWs: Left Ventricular Anterior Wall in systole. LVIDd: Left Ventricular Internal Diameter in diastole. LVIDs: Left Ventricular Internal Diameter in systole. LVPWd: Left Ventricular Posterior Wall in diastole. LVPWs: Left Ventricular Posterior Wall in systole. EF: Ejection Fraction. FS: Fractional Shortening.

[a] Statistical significance was calculated using unpaired two-tailed Student's t test, with the exception of, calculated with unpaired two-tailed Student's t test with Welch's correction

*
$p < 0.05$

**
$p < 0.01$.